Effect of Platinum Salt Concentration on the Electrospinning of Polyacrylonitrile/Platinum Acetylacetonate Solution

Zhan Lin, Mariah D. Woodroof, Liwen Ji, Yinzheng Liang, Wendy Krause, Xiangwu Zhang

Fiber and Polymer Science Program, Department of Textile Engineering, Chemistry and Science, North Carolina State University, Raleigh, North Carolina 27695-8301

Received 10 August 2009; accepted 11 October 2009
DOI 10.1002/app.31616
Published online 10 December 2009 in Wiley InterScience (www.interscience.wiley.com).

ABSTRACT: The preparation and characterization of electrospun polyacrylonitrile (PAN)/platinum(II) acetylacetonate composite nanofibers were investigated. The solution properties, such as viscosity, surface tension, and conductivity, of Pt-acetylacetonate-added PAN solutions in *N,N*-dimethylformamide were measured, and their influences on the resulting fiber structure were also determined. At low Pt salt concentrations, the addition of Pt salt increased the fiber diameter but did not change the fiber diameter distribution. However, the fiber diameter decreased, and the fiber diameter distribution became broader when the Pt salt concentration went beyond a critical value. The structure of the electrospun fibers was determined by the formation of polymer–salt–solvent interactions, which changed the balance among the viscosity, surface tension, and conductivity of the solutions.
 J Appl Polym Sci 116: 895–901, 2010

Key words: fibers; processing; nanocomposites

INTRODUCTION

Polymer fibers, with diameters ranging from tens of nanometers to several micrometers, have aroused considerable interest for various applications, such as composite systems, thin filters, and biomedical applications.[1–4] Electrospinning, which produces continuous polymer nanofibers through the action of an external electric field imposed on a polymer solution or melt, has been considered a simple and effective method for producing polymer fibers. Under an external high voltage, a pendent droplet of a polymer solution or melt at the nozzle of the spinneret becomes highly electrified, and the induced charges on the surface make the droplet deform into a Taylor cone. When the applied electric field overcomes the surface tension of the droplet, a charged stream of polymer solution or melt is ejected. The stream grows longer and thinner because of bending instability or splitting until it is deposited on the collector in the form of nanofibers.[5–7]

Electrospinning is a process involving polymer science, applied physics, fluid mechanics, and rheology.[8] The morphology of the fibers depends on the process parameters, including the applied voltage, tip-to-collector distance, and solution concentration. The fiber structure is also influenced by the addition of salt additives, which can change the solution properties, such as viscosity, surface tension, and conductivity, by the introduction of complicated polymer–salt–solvent interactions.[9,10] For example, Choi et al.[11] found that by adding small amounts of benzyl trialkylammonium chloride to poly(3-hydroxybutyrate-*co*-3-hydroxyvalerate) (PHBV) solution, they decreased the average diameter of electrospun PHBV fibers because of the change in the PHBV solution conductivity.

To date, many polymers have been electrospun to form ultrafine fibers, including poly(ethylene oxide), nylon, poly(ethylene glycol), poly(ethylene terephthalate), and polyacrylonitrile (PAN).[6,12–14] Among these polymers, PAN is a relatively tough, insoluble, and high-melting-temperature polymer with good resistances to aging, chemicals, water, and cleaning solvents; this makes it widely used in many applications, such as engineering plastics, ultrafiltration membranes, and sensors.[15–19] Moreover, PAN is also an excellent precursor for the production of carbon fibers because of its high dielectric constant, and the resulting fibers have wide applications ranging from lithium ion batteries and fuel cells to biological/chemical sensors.[20–24] Compared with other polymer carbon precursors, such as pitch and rayon, PAN-based fibers are the most suitable precursors for the production of high-performance carbon fibers because of their higher melting point and greater carbon yield.

Correspondence to: X. Zhang (xiangwu_zhang@ncsu.edu).
Contract grant sponsor: U.S. National Science Foundation; contract grant number: 0833837.
Contract grant sponsor: National Textile Center; contract grant number: ITA-08-07400.
Contract grant sponsor: American Chemical Society (ACS) Petroleum Research Fund; contract grant number: 47863-G10.

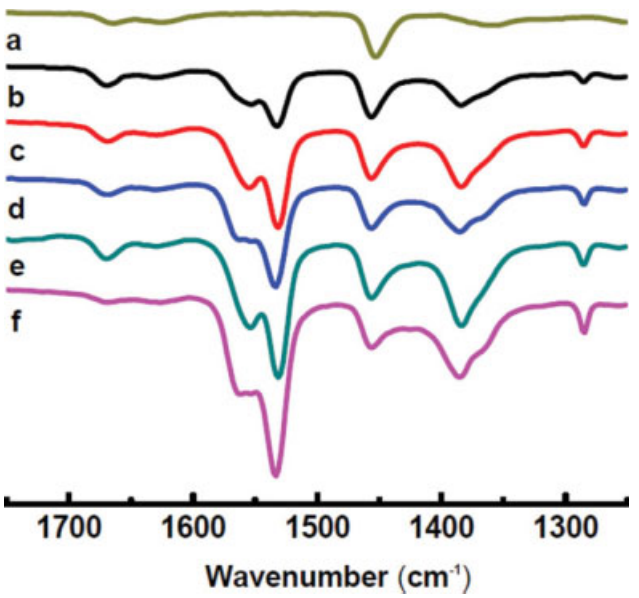

Figure 1 FTIR spectra of Pt-salt-added PAN/DMF solutions with different Pt salt concentrations: (a) 0, (b) 1.0, (c) 1.5, (d) 2.0, (e) 2.5, and (f) 3.0 wt %. [Color figure can be viewed in the online issue, which is available at www.interscience.wiley.com.]

In this article, the preparation and characterization of PAN/platinum(II) acetylacetonate [$Pt(acac)_2$] composite nanofibers by the introduction of Pt salt into a PAN/*N*,*N*-dimethylformamide (DMF) electrospinning solution are discussed. The formation of intermolecular interactions among the Pt salt, polymer, and solvent was investigated. The structure of the resulting nanofibers was controlled by the selective adjustment of the solution properties, such as viscosity, surface tension, and conductivity, through the formation of polymer–salt–solvent interactions.

EXPERIMENTAL

Chemicals and reagents

PAN (weight-average molecular weight = 150,000), DMF, and $Pt(acac)_2$ were purchased from Sigma-Aldrich (St. Louis, MO), and they were used without further purification. Deionized water was used throughout.

Solution preparation

$Pt(acac)_2$ salt was added to DMF solutions of 8 wt % PAN at 60°C with mechanical stirring for at least 5 h to form homogeneous solutions. The $Pt(acac)_2$ salt concentrations were 0, 1.0, 1.5, 2.0, 2.5, and 3.0 wt % (i.e., 0, 25.4, 38.1, 50.8, 63.5, and 76.2 μmol/g), respectively.

Solution characterization

Viscosity measurements were performed at room temperature with a TA Instruments (New Castle, DE) AR-2000 stress-controlled rheometer with primarily cone-and-plate geometry. A Fisher Scientific (Hanover Park, IL) model 21 surface tension tensiometer was used to measure the surface tension of the solutions, and a Gamry Reference 600 potentiostat (Warminster, PA) was used to measure the solution conductivity. At least six samples were used for each Pt salt concentration to ensure the reproducibility of the solution property measurements.

Electrospinning of the PAN/$Pt(acac)_2$ nanofibers

Electrospinning was conducted with a Gamma ES40P-20W/DAM variable high-voltage power supply (Ormond Beach, FL) under a voltage of 15 kV. Under high voltage, a polymer stream was ejected through a syringe and accelerated toward the nanofiber collector, during which time the solvent was rapidly evaporated. Aluminum foil was placed over the collector plate to collect the electrospun PAN/$Pt(acac)_2$ fibers.

Morphologies of the PAN/$Pt(acac)_2$ fibers

The structures of PAN and the PAN/$Pt(acac)_2$ nanofibers were evaluated with a JEOL (Tokyo, Japan) JSM-6360LV field emission scanning electron microscope at 15 kV. The electrospun samples were coated with Au/Pd layers by a Quorum Technologies K-550X sputter coater (Kent, UK) to reduce charging. We determined the diameters of the electrospun nanofibers by measuring 53 randomly selected fibers with a Revolution Systems software package (York, UK).

Fourier transform infrared (FTIR) and thermal analysis of the PAN/$Pt(acac)_2$ fibers

FTIR spectra were collected from a Nicolet Nexus 470 FTIR spectrophotometer in the wave-number range 4000–700 cm^{-1} at room temperature. We achieved adequate signal-to-noise ratios by conducting 32 scans.

Thermogravimetric analysis (TGA) was also used to determine the weight loss of the composite nanofibers at 10°C/min from 25 to 800°C in an air environment with a TA Instruments Hi-Res TGA 2950.

RESULTS AND DISCUSSION

Interactions in the Pt-salt-added PAN/DMF solutions

The interactions among PAN, DMF, and Pt salt molecules were studied by FTIR spectra (Fig. 1). Two major characteristic IR bands were found in the PAN/DMF solution at 1655 cm^{-1} for the —C=O stretching of DMF and at 1370 cm^{-1} for the —C≡N

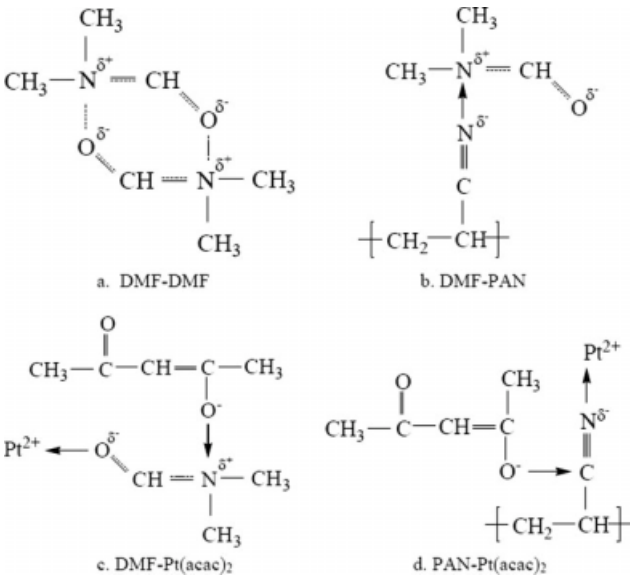

Figure 2 Schematic illustration of the interactions among PAN, DMF, and $Pt(acac)_2$ molecules in the solution.

stretching of PAN molecules. These peaks were shifted to slightly higher values when Pt salt was added to the PAN/DMF solution. For example, after the addition of Pt salt, the —C=O stretching shifted from 1662 to around 1670 cm^{-1}, and the —C≡N stretching increased from 1369 to about 1385 cm^{-1}; these changes were due to the formation of DMF–Pt salt and PAN–Pt salt complexes, respectively. Similar shifts were also found by Phadke et al.[10] for $ZnCl_2$-added PAN/DMF solutions. The shifted wave numbers of both —C=O stretching and —C≡N stretching were independent of salt concentration. Normally, there are two kinds of interactions in PAN/DMF solutions, that is, DMF–DMF [Fig. 2(a)] and DMF–PAN [Fig. 2(b)] interactions. When Pt salt molecules were introduced into the PAN/DMF solution, the Pt^{2+} and acetylacetonate ions interacted with DMF and PAN molecules; this led to the formation of two complexes [Fig. 2(c,d)], which, in turn, caused an increase in the frequency of the —C=O stretching in DMF and the —C≡N stretching in PAN.

Solution viscosity

Figure 3 shows the concentration–viscosity relationship for the Pt-salt-added PAN/DMF solutions. The solution viscosity increased with increasing Pt salt concentration and then deceased after it reached a maximum at a Pt salt concentration of 2.0 wt % (50.8 μmol/g). The changes in solution viscosity were caused by the formation of PAN–$Pt(acac)_2$ and DMF–$Pt(acac)_2$ complexes in the Pt-salt-added solutions. As shown in Figure 2, the Pt^{2+} ions had the potential to form complexes simultaneously with multiple oxygens in DMF and nitrogens in PAN, and the acetylacetonate ions strengthened the complex formation; hence, they reduced the mobilities of both PAN and DMF, which, in turn, resulted in a higher solution viscosity when the Pt salt concentration increased.[25] However, when the Pt salt concentration increased beyond 2.0 wt %, Pt^{2+} and acetylacetonate ions started to form neutral ion pairs or charged ion aggregates, which weakened the intermolecular interactions and reduced the solution viscosity. In addition, excess ions at high salt concentrations could have caused a decrease in the polymer coil dimensions. A similar effect was also reported by Shinde et al.[26] when LiCl or $ZnCl_2$ salt was added to a PAN/DMF solution. As a result, the solution viscosity (η) decreased because the viscosity was proportional to the root-mean-square-chain end-to-end distance (r), which is shown in Eq. (1):

$$\eta = \frac{K(r^2)^{3/2}}{M} \tag{1}$$

where K is a universal constant and M is the PAN polymer molecular weight (g/mol).

Solution surface tension

The surface tension, caused by the attractive intermolecular force between the molecules in the solution, played an important role in the formation of the electrospun fibers because the surface tension needed to be overcome by the applied electric field during electrospinning. Figure 4 shows the relationship between the surface tension and Pt salt concentration in the Pt-salt-added PAN/DMF solutions. When the Pt salt concentration was lower than 2.0 wt %, the surface tension increased with increasing Pt salt concentration; this was caused by the formation of DMF–

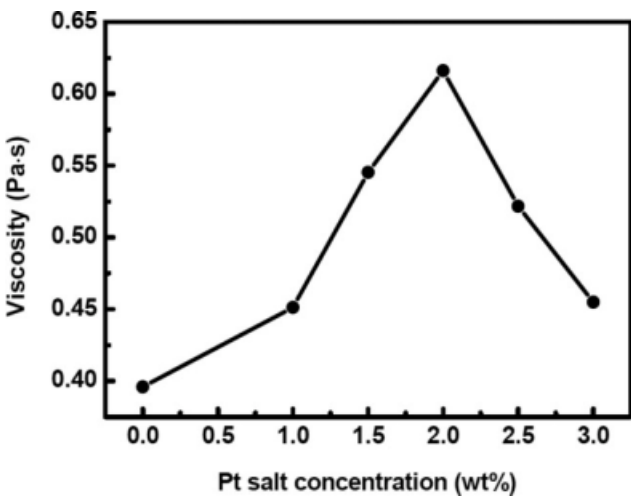

Figure 3 Relationship between the solution viscosity and Pt salt concentration for the Pt-salt-added PAN/DMF solutions.

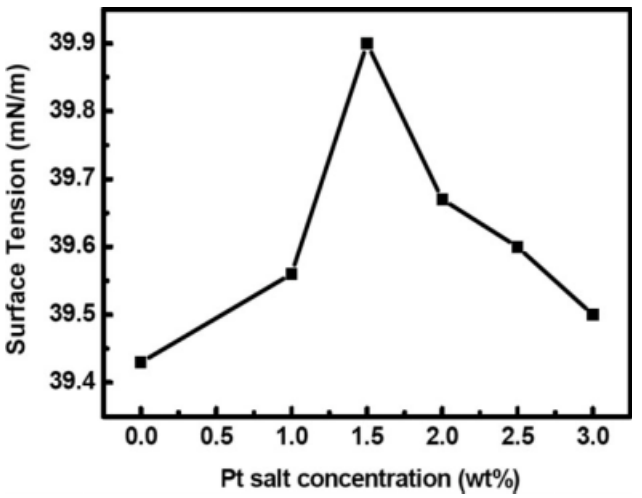

Figure 4 Relationship between the solution surface tension and Pt salt concentration for the Pt-salt-added PAN/DMF solutions.

$Pt(acac)_2$ and PAN–$Pt(acac)_2$ interactions. However, the surface tension decreased after the Pt salt concentration exceeded 2.0 wt %, which was attributable to the fact that the Pt^{2+} and acetylacetonate ions tended to form neutral ion pairs or charged ion aggregates at high salt concentrations. This may have, in turn, led to weaker intermolecular interactions in the solution and smaller surface tensions.[27]

Solution conductivity

The influence of the Pt salt concentration on the conductivity of the Pt-salt-added PAN/DMF solutions is shown in Figure 5. The solution conductivity increased with increasing Pt salt concentration, and a maximum conductivity was reached when the solution concentration was 2.5 wt %. A further increase in salt concentration led to reduced conductivity. Generally, the solution conductivity (σ) of a salt solution is governed by the following equation:

$$\sigma = \sum F z_j \mu_j c_j \tag{2}$$

where F is the Faraday constant (96485 C/mol), z_j is the charge, μ_j is the electrochemical mobility (m^2 V^{-1} s^{-1}), and c_j is the concentration (mol/L) of ion j.[28] When Pt salt was added, more Pt^{2+} and acetylacetonate ions were introduced, and hence, the solution conductivity increased. However, from Eq. (2), we also saw that the mobilities of Pt^{2+} and acetylacetonate ions also played an important role in determining the solution conductivity. When the Pt salt concentration increased beyond 2.5 wt %, the DMF–$Pt(acac)_2$ and PAN–$Pt(acac)_2$ complexes began to aggregate, which restricted Pt^{2+} and acetylacetonate ions from motion and, as a result, caused a decrease in the solution conductivity.

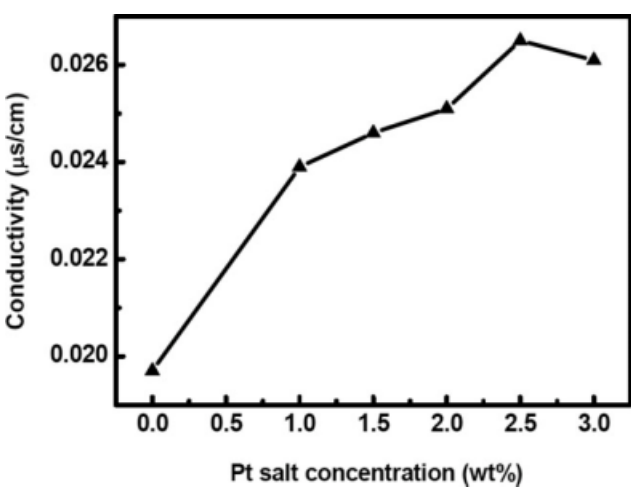

Figure 5 Relationship between the solution conductivity and Pt salt concentration for the Pt-salt-added PAN/DMF solutions.

FTIR spectra of the PAN/$Pt(acac)_2$ fibers

FTIR spectra of the PAN/$Pt(acac)_2$ composite fibers recorded in the spectral range 4000–750 cm^{-1} are shown in Figure 6. The spectrum of the pure PAN nanofibers contained prominent peaks at 2937, 2246, and 1454 cm^{-1} due to the stretching vibrations of methylene and nitrile groups and the bending vibration of methylene, respectively.[29] However, three new characteristic IR bands of PAN/$Pt(acac)_2$ composite fibers were found at 1284, 1382, and 1533 cm^{-1}, which were related to the —C—O stretching,

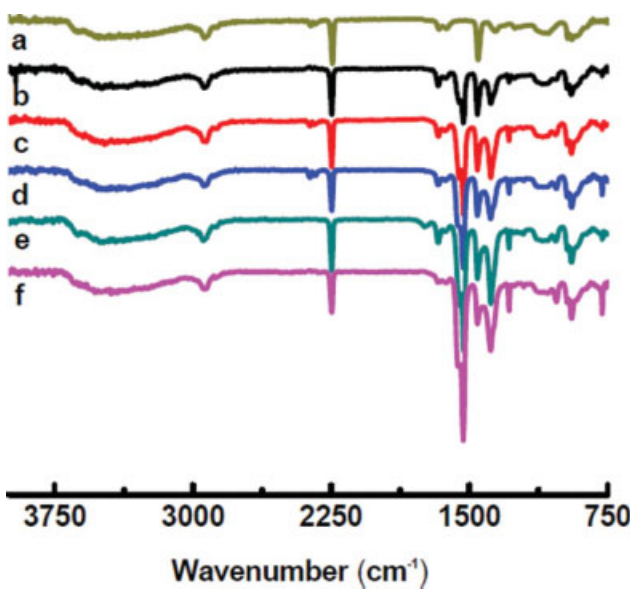

Figure 6 FTIR spectra of PAN/$Pt(acac)_2$ composite fibers with different $Pt(acac)_2$ concentrations: (a) 0 (pure PAN), (b) 1.0, (c) 1.5, (d) 2.0, (e) 2.5, and (f) 3.0 wt %. [Color figure can be viewed in the online issue, which is available at www.interscience.wiley.com.]

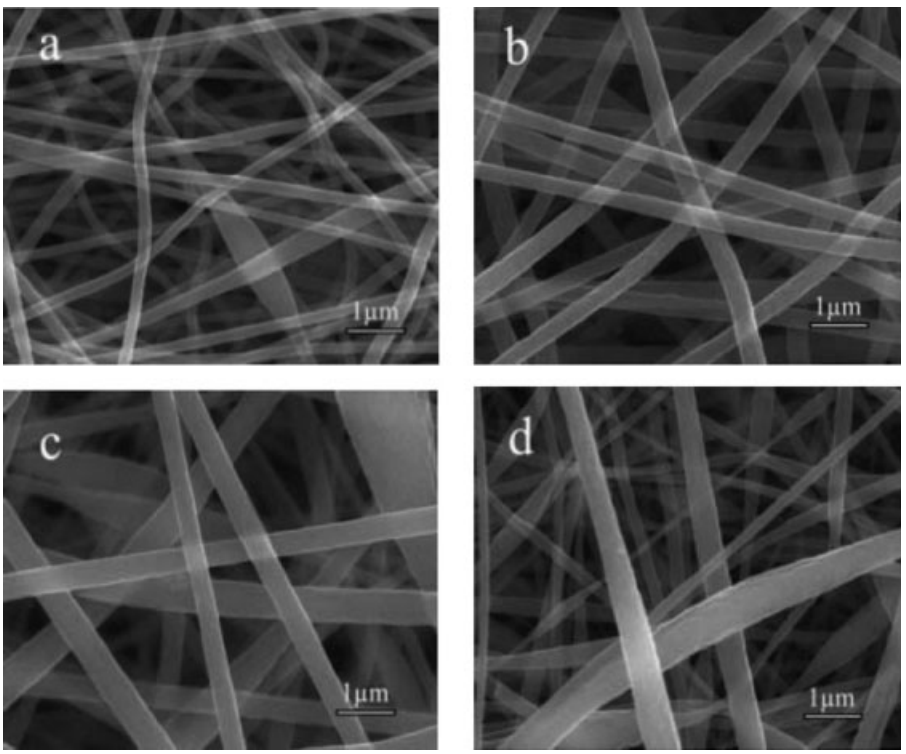

Figure 7 Scanning electron microscopy images of PAN/Pt(acac)$_2$ nanofibers prepared with different Pt salt concentrations: (a) 0, (b) 1.0, (c) 2.0, and (d) 3.0 wt %.

—CH_3 symmetrical deformation, and —C=O stretching vibrations in the Pt(acac)$_2$ salt, respectively.

Morphology of the PAN/Pt(acac)$_2$ fibers

Figures 7 and 8 show scanning electron microscopy images and diameter distributions of the PAN/Pt(acac)$_2$ nanofibers prepared with different Pt salt concentrations, respectively. The morphology of the polymer nanofibers did not change much after the addition of Pt salt. The average nanofiber diameter increased slightly from 280 to 307 to 322 nm when the Pt salt concentration increased from 0 to 1.0 to 2.0 wt %, respectively. However, when the Pt salt concentration increased to 3.0 wt %, the average fiber diameter decreased to 293 nm. In addition, the diameter distribution of the composite nanofibers became much boarder at a Pt salt concentration of 3.0 wt %.

During electrospinning, a higher solution viscosity typically leads to a larger fiber diameter because of the greater resistance of the solution to be stretched by the charges in the electrospun jet, and an increase in the conductivity results in a smaller diameter because of the increase in the stretching of the jet. A suitable surface tension is also needed to obtain uniform fibers.[30,31] As shown in Figures 3–5, when the salt concentration increased from 0 to 2.0 wt %, the change in the solution viscosity was significant (an increase of 25%), but those of the surface tension and conductivity were only 0.3 and 12%, respectively. Therefore, at low Pt salt concentrations, the increasing viscosity was the dominant reason for the electrospun PAN/Pt(acac)$_2$ nanofibers to have larger diameters when the Pt salt concentration increased. For a similar reason, the fiber diameter decreased at high Pt salt concentrations because the decrease in the viscosity (13%) was significantly larger than the decrease in surface tension (0.2%) and the increase of conductivity (4%) when the salt concentration increased from 2.0 to 3.0 wt %.

To obtain uniform fibers, a high solution conductivity is desired because the electrostatic repulsion must overcome the surface tension of the solution at the tip of the spinneret. It is also easier to obtain a steady jet without splitting if the solution viscosity is relatively large. When the Pt salt concentration reached 3.0 wt %, the relatively large decrease (15%) in the solution viscosity resulted in unsteady jets and, hence, the splitting of the fibers during electrospinning, which was responsible for the broader distribution of the fiber diameters at the high Pt salt concentration of 3.0 wt %.

Thermal analysis of the PAN/Pt(acac)$_2$ nanofibers

Thermal studies of the PAN/Pt(acac)$_2$ nanofibers were carried out with TGA in an air atmosphere (Fig. 9). Compared with the pure PAN nanofibers,

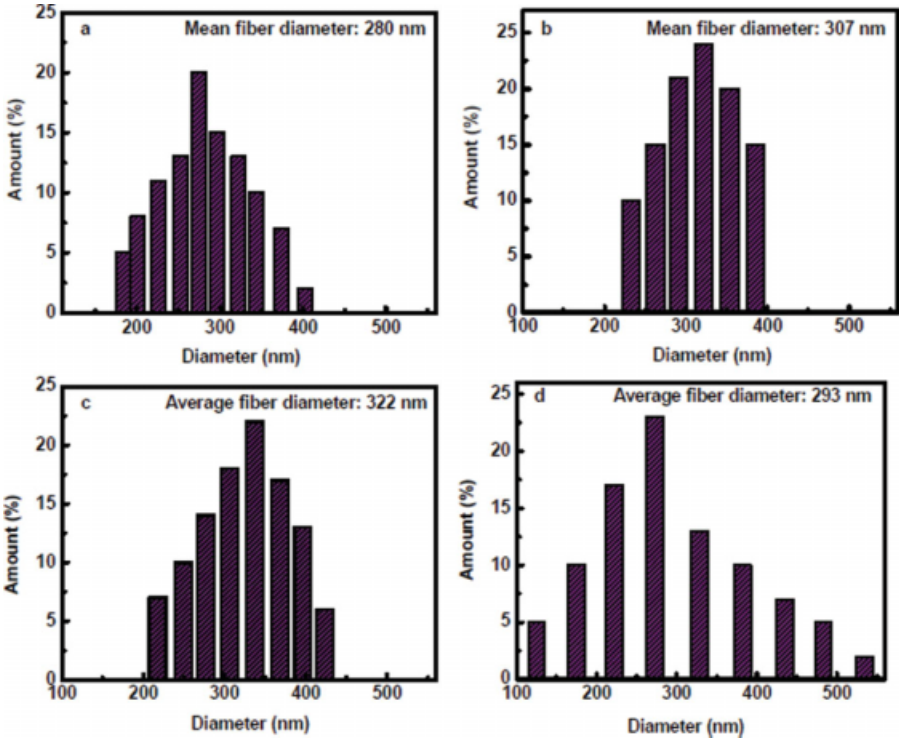

Figure 8 Diameter distributions of PAN/Pt(acac)$_2$ nanofibers prepared with different Pt salt concentrations: (a) 0, (b) 1.0, (c) 2.0, and (d) 3.0 wt %. [Color figure can be viewed in the online issue, which is available at www.interscience.wiley.com.]

which degraded around 320°C, the PAN/Pt(acac)$_2$ nanofibers began losing weight at a lower temperature of around 200°C, which was due to the decomposition of Pt(acac)$_2$ in the composite nanofibers. The decomposition of Pt salt also destroyed their interactions with the PAN chains and accelerated the oxidative reactions of the PAN nanofibers, which resulted in the lower decomposition temperature of PAN in the PAN/Pt(acac)$_2$ nanofibers.[32]

Detailed information on the decomposition of the PAN/Pt(acac)$_2$ nanofibers between 675 and 800°C is shown in the inset of Figure 9. As shown, the final weight percentage of the pure PAN nanofibers was almost zero; this meant that the PAN nanofibers completely decomposed in the air. However, the final weight percentage of the PAN/Pt(acac)$_2$ composite nanofibers did not reach zero because of the leftover Pt particles after the decomposition of the Pt(acac)$_2$ salt. When an inert environment is used during the heat treatment, PAN can transfer to carbon.[20–24] This opens up opportunities for producing Pt-particle-loaded carbon nanofibers for various applications, such as fuel cells, sensors, and catalysts.

CONCLUSIONS

We prepared PAN/Pt(acac)$_2$ composite nanofibers with well-defined morphologies by electrospinning Pt-salt-added PAN/DMF solutions. At low Pt salt concentrations, the addition of Pt salt increased the fiber diameter because of the predominant influence of the increasing solution viscosity; however, the fiber diameter decreased at higher Pt salt concentrations because of the decreased solution viscosity and

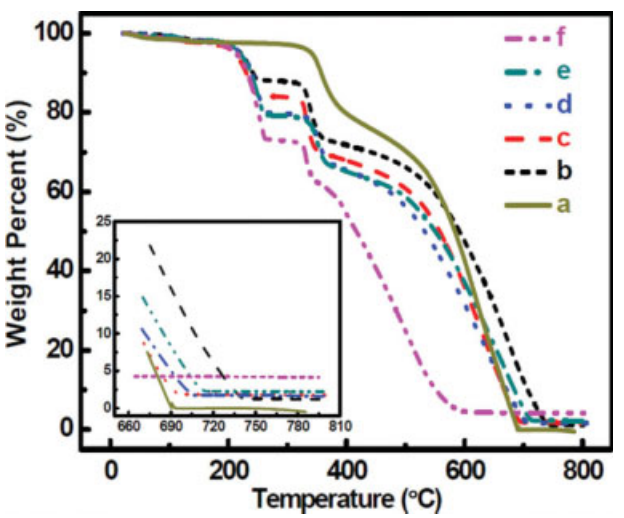

Figure 9 TGA thermograms of PAN/Pt(acac)$_2$ composite nanofibers with different Pt salt concentrations: (a) 0 (pure PAN), (b) 1.0, (c) 1.5, (d) 2.0, (e) 2.5, and (f) 3.0 wt %. Inset: Detailed information of the decomposition between 675 and 800°C. [Color figure can be viewed in the online issue, which is available at www.interscience.wiley.com.]

increased solution conductivity. The FTIR results confirm the formation of the interactions among the Pt salt, PAN, and DMF, and the TGA data showed a decreased thermal stability of the PAN/$Pt(acac)_2$ composite nanofibers compared with the pure PAN nanofibers; this resulted from the decomposition of Pt salt in the composite nanofibers.

References

1. Bergshoef, M. M.; Vancso, G. J. Adv Mater 1999, 11, 1362.
2. Gibson, P.; Rivin, D.; Kendrick, C.; Schreuder-Gibson, H. Text Res J 1999, 69, 311.
3. Huang, L.; McMillan, R. A.; Apkarian, R. P.; Pourdeyhimi, B.; Conticello, V. P.; Chaikof, E. L. Macromolecules 2000, 33, 2989.
4. Kim, J. S.; Reneker, D. H. Polym Compos 1999, 20, 124.
5. Deitzel, J. M.; Kleinmeyer, J.; Harris, D.; Tan, N. C. B. Polymer 2001, 42, 261.
6. Jaeger, R.; Bergshoef, M. M.; Batlle, C. M. I.; Schonherr, H.; Vancso, G. J. Macromol Symp 1998, 127, 141.
7. Reneker, D. H.; Yarin, A. L.; Fong, H.; Koombhongse, S. J Appl Phys 2000, 87, 4531.
8. Gu, S. Y.; Ren, J.; Vancso, G. J. Eur Polym J 2005, 41, 2559.
9. Lee, H. J.; Won, J.; Lee, H.; Kang, Y. S. J Membr Sci 2002, 196, 267.
10. Phadke, M. A.; Musale, D. A.; Kulkarni, S. S.; Karode, S. K. J Appl Polym Sci 2005, 43, 2061.
11. Choi, J. S.; Lee, S. W.; Jeong, L.; Bae, S. H.; Min, B. C.; Youk, J. H.; Park, W. H. Int J Biol Macromol 2004, 34, 249.
12. Fennessey, S. F.; Farris, R. J. Polymer 2004, 45, 4217.
13. Gibson, P. W.; Schreuder-Gibson, H. L.; Rivin, D. AIChE J 1999, 45, 190.
14. Norris, I. D.; Shaker, M. M.; Ko, F. K.; MacDiarmid, A. G. Synth Met 2000, 114, 109.
15. Perera, K. S.; Dissanayake, M. A. K. L.; Skaarup, S.; West, K. J Solid State Electrochem 2008, 12, 873.
16. Gupta, S.; Ou, R. Q.; Gerhardt, R. A. J Electron Mater 2006, 35, 224.
17. Kim, I. C.; Yun, H. G.; Lee, K. H. J Membr Sci 2002, 199, 75.
18. Rahaman, M. S. A.; Ismail, A. F.; Mustafa, A. Polym Degrad Stab 2007, 92, 1421.
19. Shan, D.; Wang, S. X.; He, Y. Y.; Xue, H. G. Mater Sci Eng C 2008, 28, 213.
20. Cho, T. H.; Sakai, T.; Tanase, S.; Kimura, K.; Kondo, Y.; Tarao, T.; Tanaka, M. Electrochem Solid-State Lett 2007, 10, A159.
21. Gao, X. P.; Bao, J. L.; Pan, G. L.; Zhu, H. Y.; Huang, P. X.; Wu, F.; Song, D. Y. J. Phys Chem B 2004, 108, 5547.
22. Guo, J. S.; Sun, G. Q.; Wang, Q.; Wang, G. X.; Zhou, Z. H.; Tang, S. H.; Jiang, L. H.; Zhou, B.; Xin, Q. Carbon 2006, 44, 152.
23. Jang, J.; Bae, J Sens Actuators B 2007, 122, 7.
24. Ji, L. W.; Zhang, X. W. Nanotechnology 2009, 20.
25. Du, J. M.; Zhang, X. W. J Appl Polym Sci 2008, 109, 2935.
26. Shinde, M. H.; Kulkarni, S. S.; Musale, D. A.; Joshi, S. G. J Membr Sci 1999, 162, 9.
27. Bruce, P. G.; Vincent, C. A. J Chem Soc Faraday Trans 1993, 89, 3187.
28. Bohnke, O.; Frand, G.; Rezrazi, M.; Rousselot, C.; Truche, C. Solid State Ionics 1993, 66, 97.
29. Yue, Z. R.; Benak, K. R.; Wang, J. W.; Mangun, C. L.; Economy, J. J Mater Chem 2005, 15, 3142.
30. Jarusuwannapoom, T.; Hongroijanawiwat, W.; Jitjaicham, S.; Wannatong, L.; Nithitanakul, M.; Pattamaprom, C.; Koombhongse, P.; Rangkupan, R.; Supaphol, P. Eur Polym J 2005, 41, 409.
31. Zong, X. H.; Kim, K.; Fang, D. F.; Ran, S. F.; Hsiao, B. S.; Chu, B. Polymer 2002, 43, 4403.
32. Dalton, S.; Heatley, F.; Budd, P. M. Polymer 1999, 40, 5531.